

Review

Protection Circuit Design for Ultrasound Transducers

Hojong Choi

Department of Electronic Engineering, Gachon University, 1342 Seongnam-daero, Sujeong-gu, Seongnam 13120, Republic of Korea; hojongch@gachon.ac.kr; Tel.: +82-31-750-5591

Abstract: In ultrasound systems, a protection circuit must be used to protect the receiver electronics from the high-voltage pulses generated by the transmitter and to minimize the signal loss and distortion of the low-voltage echoes generated by the transducer. Especially for certain ultrasound applications, such as intravascular ultrasound, particle manipulation, and cell stimulation, proper performance of the ultrasound transducers is desirable due to their low sensitivity. As the operating frequency of the ultrasound transducer increases, the size of the transducer decreases, increasing the amplitude of the transmitted signals to achieve proper acoustic performance. In such environments, a protection circuit can be used to protect the receiver electronics in ultrasound systems. To design suitable protection circuits, transistors, resistors, capacitors, and inductors are used, and the parameters of insertion loss, noise, total harmonic distortion, and recovery time of the protection circuits must be carefully considered. Various approaches have been developed to protect circuits such as transmission lines, transformers, bridge diodes, and metal-oxide-semiconductor field-effect transistor devices. Certain protection circuits are beneficial for impedance matching and area reduction. Other protection circuits have been designed to increase bandwidth, reduce insertion loss, or improve the signal-to-noise ratio for different ultrasound applications. Therefore, this review article may be useful for academic ultrasound researchers or circuit designers in selecting appropriate protection circuit types for specific ultrasound transducer applications.

Keywords: protection circuit; ultrasound transducer; ultrasound system



Academic Editor: Alessandro Lo Schiavo

Received: 19 January 2025

Revised: 13 February 2025

Accepted: 16 February 2025

Published: 18 February 2025

Citation: Choi, H. Protection Circuit Design for Ultrasound Transducers. *Appl. Sci.* **2025**, *15*, 2141. <https://doi.org/10.3390/app15042141>

Copyright: © 2025 by the author. Licensee MDPI, Basel, Switzerland. This article is an open access article distributed under the terms and conditions of the Creative Commons Attribution (CC BY) license (<https://creativecommons.org/licenses/by/4.0/>).

1. Introduction

In medical ultrasound imaging systems, the transmitter, receiver, and transducer are the three main electronic and mechanical components [1,2]. In ultrasound systems, the transducer should be located between the transmitter and receiver [3]. High-voltage pulse signals generated by the transmitter trigger the transducer to generate acoustic signals from the desired sample target [4,5]. The received acoustic signals are converted into electrical echo signals using a transducer [6]. Before the echo signals are received by the transducer, high-voltage pulse signals reach the receiver electronics because of the shared paths between the transmitter and receiver [7,8].

Figure 1 shows the signal path between the transmitter/receiver and the transducer to describe the fundamental mechanism of the transmitted pulse and the received echo. First, the transmitted pulse signals are passed through the expander to the transducer. Typically, an expander circuit is used to remove the ring-down of the transmitted high-voltage pulse signals while minimizing the reduction in the transmitted pulse amplitude [9]. An acoustic wave is transmitted from the transducer to the desired sample. The received acoustic waves are converted using a transducer. Secondly, the discharged pulse signal travels to the limiter before the electrically reflected echo reaches the limiter. Third, a limiter circuit was used to

suppress the discharged pulse and pass the reflected echo before it reaches the receiver [10]. Therefore, a limiter circuit is used to suppress the discharged pulse while minimizing the reduction in the reflected echo. In diagnostic ultrasound imaging applications, one or two pulses are usually used to obtain a wide bandwidth [11]. For Doppler imaging and cell or particle stimulation applications, multicycle pulses are generally used, which provide more stress to the receiver electronics to obtain a narrow bandwidth [12].

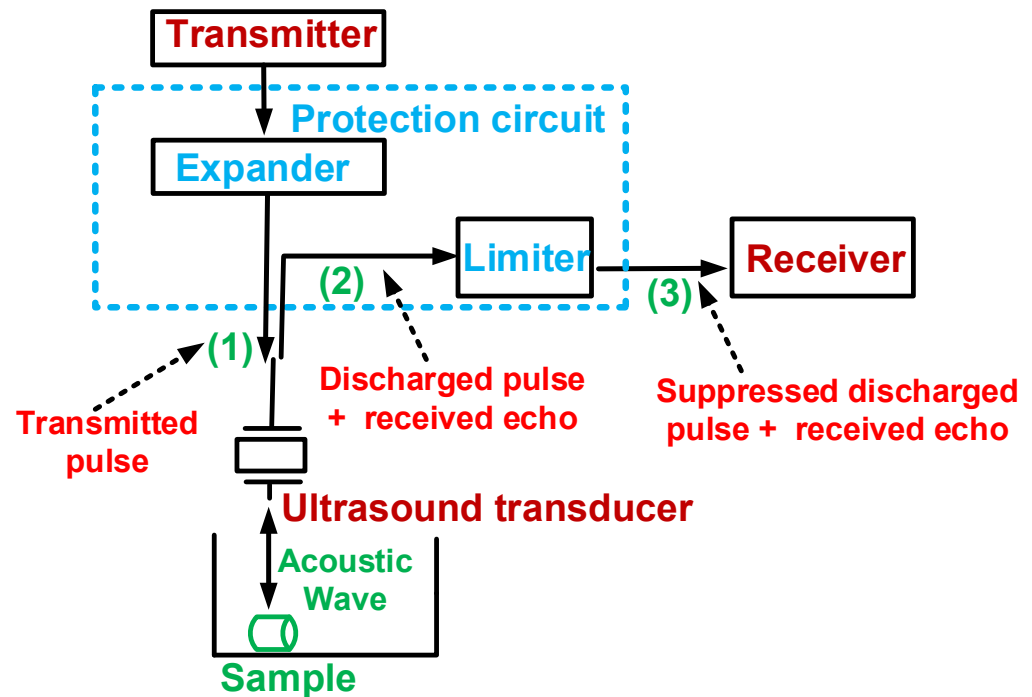


Figure 1. Description of the signal path when the protection circuit is located with the transmitter, receiver, and transducer.

Pulse signals must be used to trigger the ultrasound transducers. However, as the operating frequency of the ultrasound transducers increases, their size decreases, which reduces their sensitivity [13,14]. In addition, the transmitted voltage applied to the ultrasound transducer must be elevated [15]. Therefore, proper selection of the protection circuit for operating high-frequency or very high-frequency transducers is important for optimal ultrasound system performance.

First, several database search engines, such as Google Scholar, MedLine, PubMed, Embase, ProQuest, and EBSCOhost, were used to find suitable research articles on protection circuits for medical ultrasound systems. Second, duplicate articles were excluded from the analysis. The titles, introductions, methods, abstracts, and conclusions of each research article were reviewed to identify the specific design topologies, parameter specifications, and performances. Articles in which the specific design topology of the protection circuits was not presented were removed. The selected articles were examined in this review paper.

The rest of this paper is organized as follows: Section 2 describes the general design topology and the specific design parameters, Section 3 presents detailed design concepts for different transducer applications and describes how to select such protection circuits for specific ultrasound applications, Section 4 discusses currently developed protection circuits used for ultrasound transducer applications; this allows academic researchers to determine the selection of protection circuits for ultrasound research, and Section 5 provides the conclusions and a summary of this review.

2. Fundamental Concepts and Parameters of the Protection Circuits

The protection circuit consists of expander and limiter circuits. Figure 2 shows the operating mechanisms of the expander and limiter. In the ultrasound system, the transmitter is usually a pulser or a power amplifier used to generate the transmitted pulse, and the receiver is a preamplifier with a variable-gain amplifier or a time-gain compensation amplifier [16].

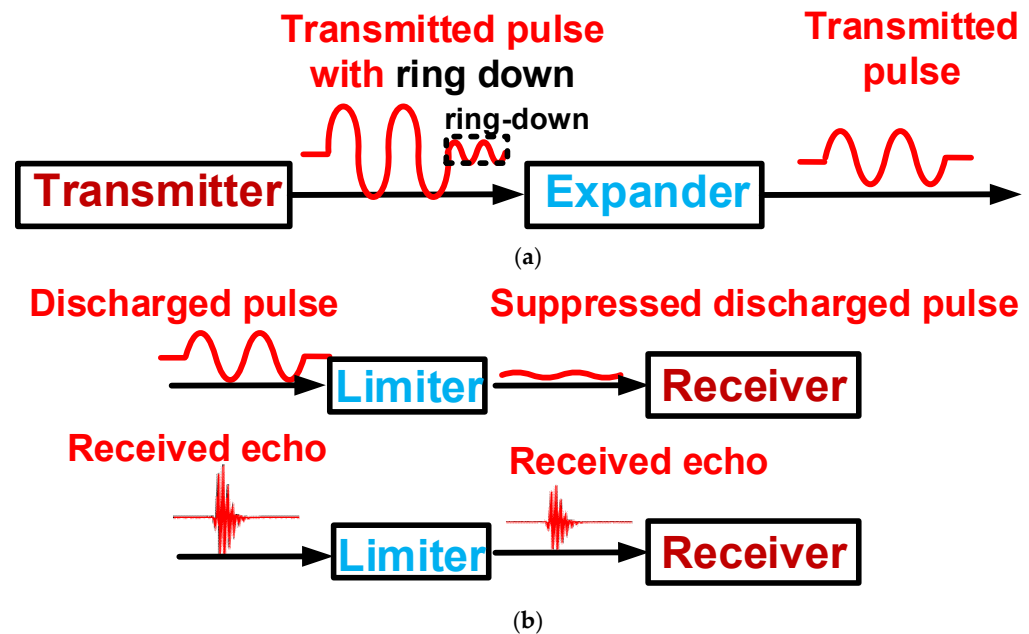


Figure 2. Operating mechanism of the (a) expander and (b) limiter in the protection circuits.

As shown in Figure 2a, the expander circuit is used to suppress the ring-down of the transmitted signals generated while minimizing the signal loss from the transmitter [17]. The reason for this is that the ring-down signal can aggravate the signal distortion caused by the voltage applied to the transducer. Therefore, unwanted harmonic distortion may be amplified in the received echo. As shown in Figure 2b, a limiter circuit, which is the main component of the protection circuit, has been used to suppress the discharged pulses and protect the receiver. Meanwhile, the received echo must be passed through with good signal integrity, with minimum loss or distortion.

The core parameters of the protection circuit are the insertion loss (IL), harmonic distortion or total harmonic distortion (THD), noise figure (NF), input-referred noise, bandwidth, and recovery time. The IL is obtained by dividing the original signal from the protection circuit by the passed signal without the protection circuit, as shown in Equation (1) [18–20].

$$IL(\text{dB}) = 20 \cdot \text{Log}_{10} \left(\frac{\text{output with protection circuit}}{\text{output without protection circuit}} \right) \quad (1)$$

The IL parameter is an important advantage because the protection circuit is located in the first-stage receiver electronics. Therefore, a low IL value in the circuit can affect the noise performance of the receiver. Equation (2) describes the general NF of an analog receiver circuit [21,22]. If a passive device has only one loss, the gain is inversely proportional to the loss [23]. Therefore, Equation (2) changes to Equation (3).

$$NF_{\text{total}} = NF_1 + \frac{NF_2 - 1}{G_1}, \quad (2)$$

where NF_{total} , NF_1 , and NF_2 are the total NF of the protection circuit and receiver, NF of the protection circuit, and NF of the receiver, respectively, and G denotes the gain of the protection circuit.

$$NF_{total} = NF_1 + L_1(NF_2 - 1), \quad (3)$$

where L_1 is the loss of the protection circuit.

Equation (3) shows that the NF_{total} can be dependent on the NF_1 and L_1 :

The high signal distortion of the protection circuit can increase the ring-down of the discharged pulses and the harmonic distortion of the obtained echo signals. The THD for the protection circuit can be calculated using Equation (4) [24–26].

$$\begin{aligned} \text{THD(dB)} &= 20 \cdot \text{Log}_{10} \left(\frac{V_2^2 + V_3^2 + V_4^2 + \dots + V_n^2}{V_1^2} \right) \\ \text{THD(\%)} &= \left(\frac{V_2^2 + V_3^2 + V_4^2 + \dots + V_n^2}{V_1^2} \right) \cdot 100 \end{aligned} \quad (4)$$

where V_1 , V_2 , V_3 , V_4 , and V_n are the amplitudes of the fundamental, the 2nd harmonic, the 3rd harmonic, the 4th harmonic, and the n th harmonic signals of the protection circuit, respectively.

In the limiter circuit, the discharged pulse signal must be suppressed as much as possible to prevent the echo signal from affecting the performance of the receiver. A relatively short recovery time for the discharged pulse is desirable when an echo signal with a long duration is obtained. The recovery time of the protection circuit is defined by Equation (5) [27–29].

$$\text{Recovery time (s)} = T_{fall} - T_{start}, \quad (5)$$

where T_{fall} is the first time in which the discharged pulse of the protection circuit reaches a certain $\pm 1\%$ or 10% points of the final pulse, and T_{start} is the first time in which the discharged pulse of the protection circuit starts certain rise/fall points of the final pulse.

The echo signal received from the ultrasound transducer must be passed with a minimum IL, harmonic distortion, and noise figure or input-referred noise without affecting the bandwidth. The bandwidth of the protection circuit also must be greater than that of the echo generated by the transducer. Certain types of protection circuits are undesirable for very high frequency (>100 MHz) ultrasound transducer applications.

3. Design Topology and Analysis of the Developed Protection Circuits

This section describes the topology and analysis of previously developed protection circuits for ultrasound transducers or system applications. In addition, the specific parameters and the achieved performance of the protection circuits are described. In the analysis, the blocks of the transmitter, receiver, and protection circuit with the transducer were shown to emphasize the design topology of the protection circuit.

Different labels and designs in each paper are shown in the schematic design. Identical designations and symbols were used for the resistor, capacitor, diode, transistor, and supply voltage so that the schematic designs of the protective circuits can be easily compared. The resistor, capacitor, and diode are selected as R , C , and D , the transformer is selected as T , and the N-channel and P-channel transistors are selected as “N” and “P”, respectively. In addition, all protection circuit designs have been redrawn to facilitate comparison. Therefore, academic researchers can help select the types of protection circuits that are beneficial for ultrasound transducer research.

Figure 3 shows the protection circuit developed by Lockwood et al. [30]. The expander typically consists of a single-series cross-coupled diode pair (D_1 and D_2), and the limiter consists of a transmission line with a parallel cross-coupled diode pair (D_3 and D_4). The transmission line is used to match the impedance of the receiver for certain frequency

ranges such as 30–35 or 40–45 MHz. The impedance of the transmission line depends on its length [31]. Thus, a suitable length for specific operating frequencies must be selected for impedance matching [32,33]. Lockwood et al. have implemented the transmission line with a 20 cm step from 20 cm to 0.2 m for a 45 MHz polyvinylidene difluoride (PVDF) ultrasound transducer [30].

When high-voltage bipolar pulses pass through a transmission line, the diodes (D_3 and D_4) should have low impedance so such discharged pulses can reach the ground. However, when low-voltage echoes are passed through a transmission line, the p-n diodes (D_3 and D_4) should have a high impedance so that the echoes reach the receiver with a small IL.

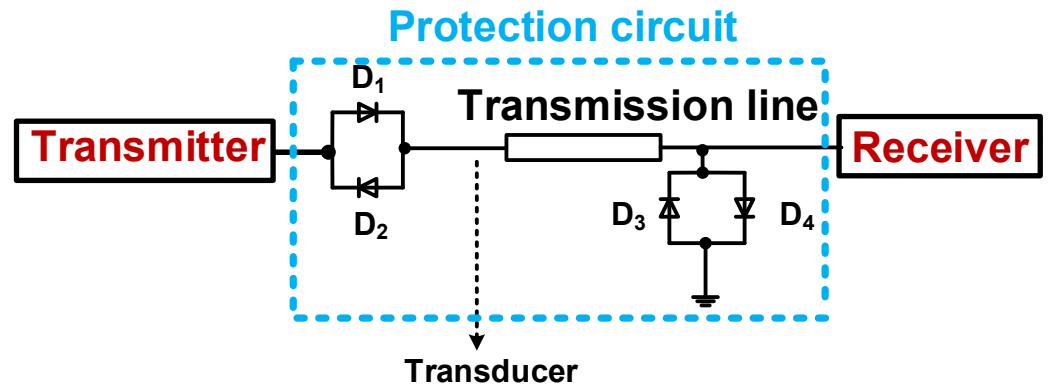


Figure 3. Protection circuit for 45 MHz PVDF ultrasound transducer. Adapted with permission from Lockwood et al. [30]. Copyright 1991, IEEE.

Figure 4 shows a duplexer design with a variable capacitive diode for an ultrasound imaging system [34]. Variable capacitive diodes (D_3 and D_4) with opposite directions were used to separate the pulses and echoes while minimizing the IL and noise contributions. Variable capacitive diodes operate in the reverse direction for positive and negative pulses. The pin diode (D_5) has a conducting voltage of 0.7 V. The resistor (R_1) was attached to a bipolar transistor in the receiver [34].

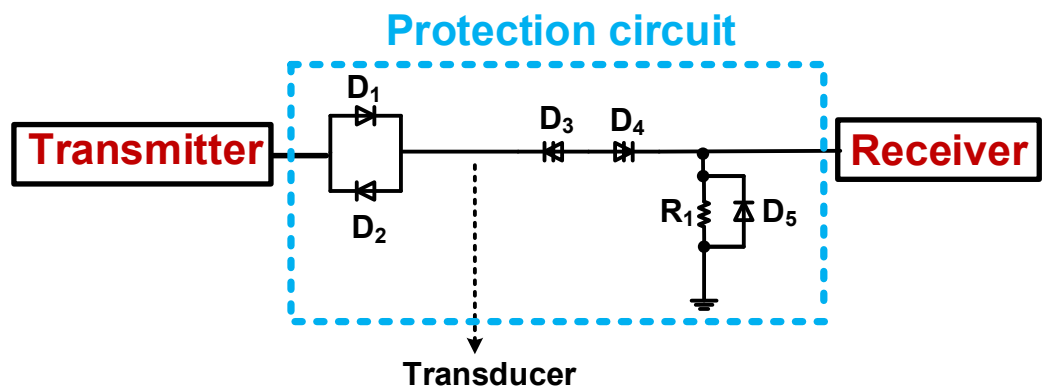


Figure 4. The protection circuit is based on variable capacitive diodes for ultrasound imaging systems [34].

Figure 5 shows the protection circuit with diodes and a transformer (T_1) [35]. The bridge diodes ($D_3, D_4, D_5,$ and D_6) operate on the basis of the direct current (DC) bias voltages (S_1 and S_2). The transmitted bipolar pulses could be coupled to the ground via the parallel diode pair (D_7 and D_8). A transformer is typically used to block a DC signal and pass an AC signal [36,37]. The primary and secondary coils are connected to the receiver and transducer, respectively; therefore, an unwanted DC source to the transducer is blocked.

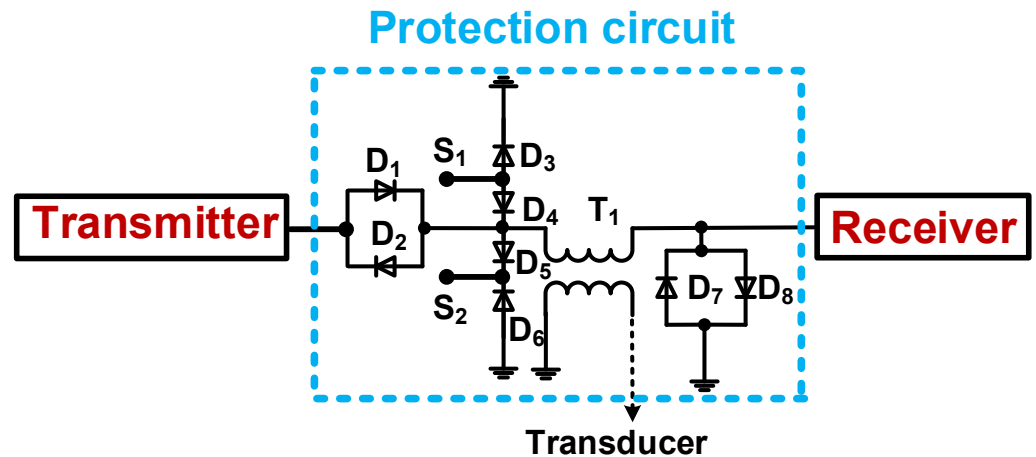


Figure 5. Schematic design of the protection circuit based on a bridge diode and a transformer [35].

Figure 6 shows an expander- and a transformer-based limiter for a high-frequency ultrasound imaging system developed by Poulsen [38]. A transformer with a wide bandwidth was used to reduce the IL for high-frequency operations. In addition, a transformer with a 1–N ratio (T_1) could be useful to reduce the large amplitude current to reduce the stress on the receiver. This transformer can extend the pulse duration of the echo generated by a high-frequency ultrasound transducer owing to its nonlinear characteristics [38]. The resistor (R_1) can be helpful to be matched to the receiver with a $50\ \Omega$ termination and reduced high-voltage pulses. The ILs of the developed protection circuit were -4 to -8 dB at 20 MHz and -55 to -66 dB at 45 MHz. When using a 20 MHz transducer, a center frequency of 20.5 MHz and a bandwidth of 21.6 MHz were achieved. When using a 45 MHz transducer, a center frequency of 46.6 MHz and a bandwidth of 34.7 MHz were also achieved [38].

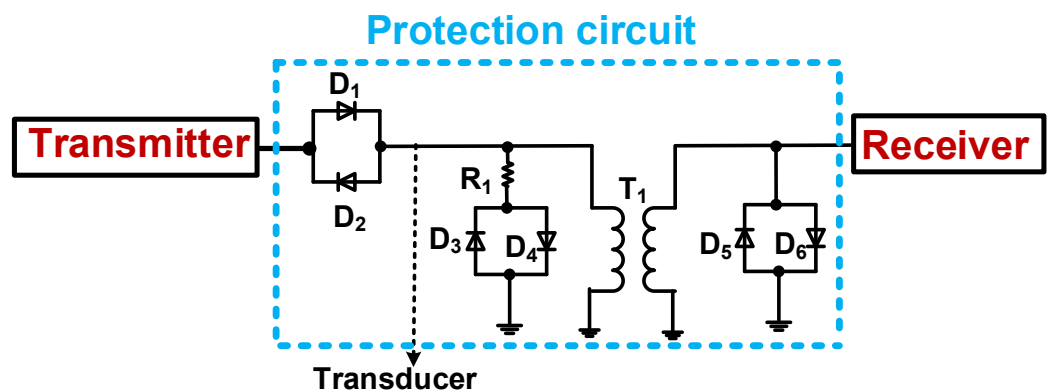


Figure 6. Schematic representation of the expander and transformer-based limiter. Adapted with permission from Poulsen [38]. Copyright 1999, IEEE.

As shown in Figure 7, Vogt et al. have developed a protection circuit that is an expander and limiter consisting of a bridge diode connection with a transmission line to improve image resolution for high-frequency ultrasound skin-imaging applications. The impedances of the bridge diodes (D_3 , D_4 , D_5 , and D_6) are controlled by the resistance values (R_1 and R_2), which must be selected accordingly. In addition, a suitable length of the transmission line could improve the impedance-matching condition. Therefore, the configuration can influence the IL and bandwidth of the protection circuit. When high-voltage pulses are transmitted to the transducer, the expander operates at a low impedance, but the limiter operates at a high impedance to protect the receiver. When low-voltage echoes are received from the transducer, the supply voltage ($\pm V_{dd}$) can provide a DC

voltage through the resistors (R_1 and R_2) to conduct the diodes (D_3 , D_4 , D_5 , and D_6), which should have a low impedance. When positive transmitted pulses go to the bridge diode, diode (D_5) is conducted and diode (D_6) suppresses the positive pulses. When negatively transmitted pulses reach the bridge diode, the diode (D_3) is conducted, and the diode (D_4) suppresses the negative pulses. The measured ILs of the expander and limiter at 150 MHz were approximately -10 dB and -15 dB, respectively. The signal distortion improved by 19 dB.

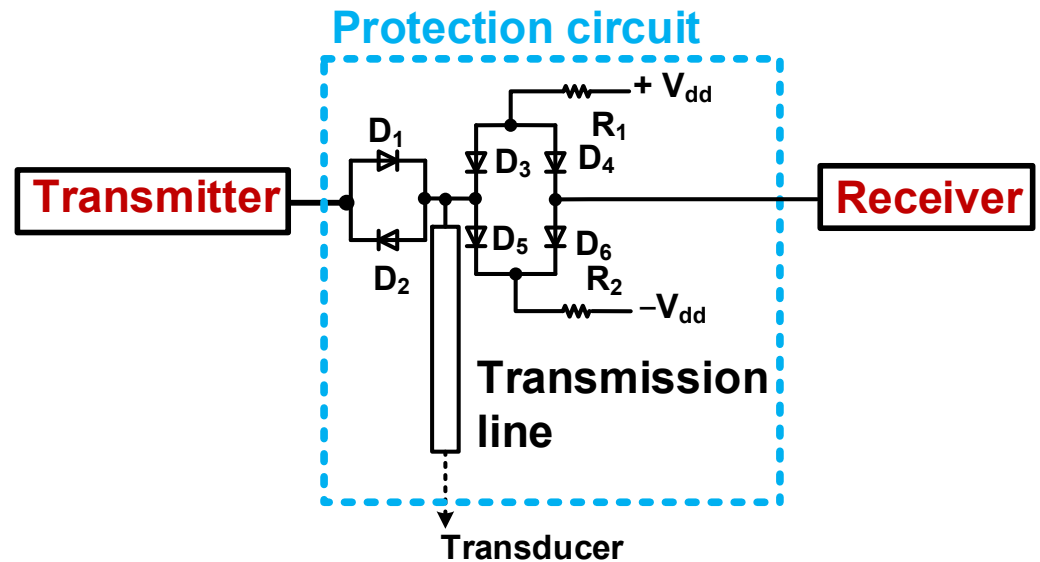


Figure 7. Schematic representation of the protection circuit used for the high-frequency ultrasound skin imaging system. Adapted with permission from Vogt et al. [39]. Copyright 2003, IEEE.

Figure 8 shows a protection circuit based on a double-bridge diode configuration for ultrasound catheter applications. An ultrasound catheter is a type of rotational ultrasound transducer used in intravascular ultrasound (IVUS) systems [40,41]. A dual-diode bridge was used to protect the input and output of the preamplifier used in the receiver. The DC bias voltages from the power supply ($+V_{dd}$) turned on the bridge diodes. A long coaxial cable must be used for the IVUS system; impedance matching is important. The values of capacitance (C_1 and C_2) and resistance (R_1 and R_2) can influence the impedance, bandwidth, and IL of the bridge diodes. Therefore, the proper selection of these values in the bridge diode configuration is essential for the transducer performance.

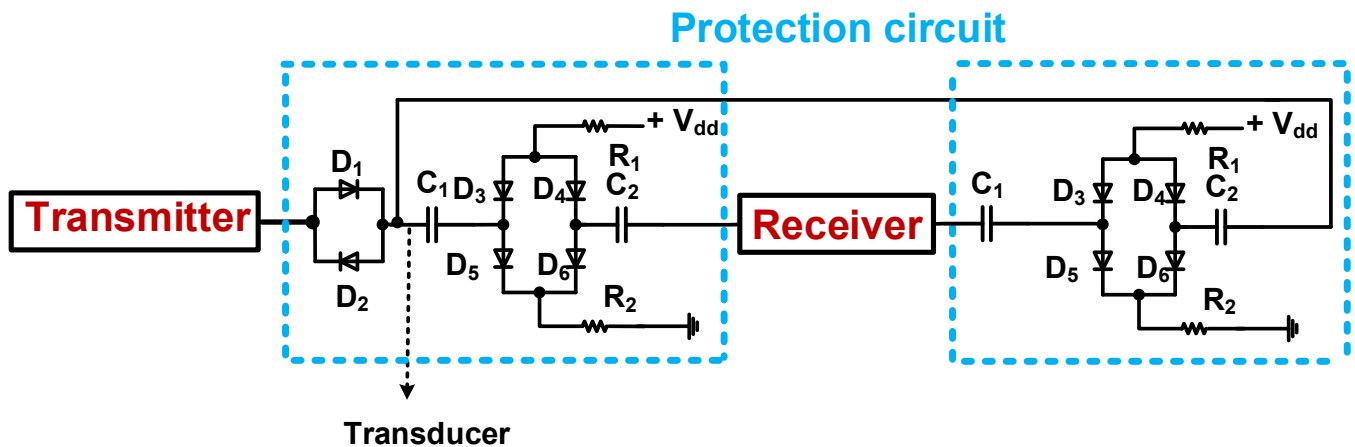


Figure 8. Schematic representation of the protection circuit based on double bridge diode configuration. Adapted with permission from Moore et al. [42]. Copyright 2003, IEEE.

As shown in Figure 9, Fuller et al. proposed a 64-channel on-chip Metal-oxide-semiconductor field-effect transistor (MOSFET) shunt device for protection circuits. Instead of high-voltage switches, the authors used a standard low-voltage 0.35- μm complementary metal-oxide-semiconductor (CMOS) process to reduce the cost of portable high-channel ultrasound imaging system applications. The transducer is connected to the positive side of the receiver, and a common-mode DC voltage (V_{CM}) of 1.5 V is connected to the negative side of the receiver. During the transmission period, a high-voltage switch (S_1) is switched on. During the receiving period, the MOSFET shunt device (S_2) is turned on. The measured discharged pulse voltage was approximately 1.1 $V_{\text{p-p}}$ when a transmit pulse of 10 $V_{\text{p-p}}$ with a pulse period of 250 ns was applied.

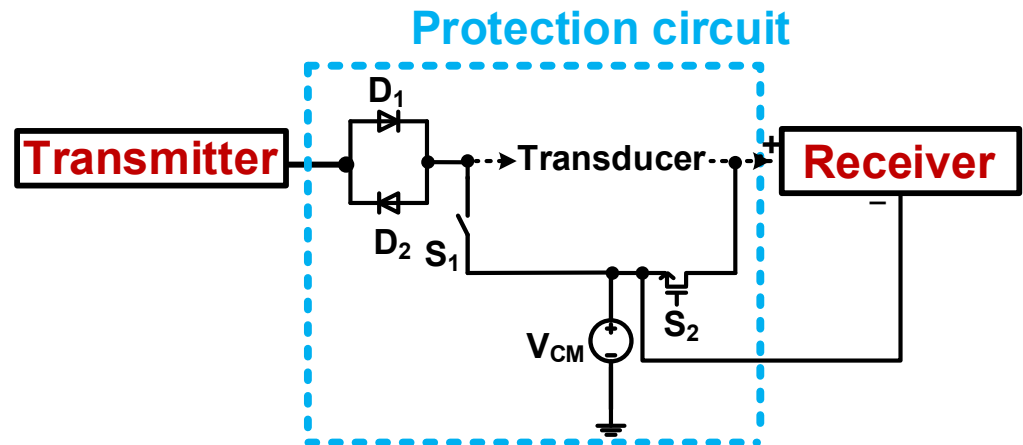


Figure 9. Schematic representation of the protection circuit using a common-mode DC voltage (only one connection is shown to simplify the analysis). Adapted with permission from Fuller et al. [43]. Copyright 2007, IEEE.

Figure 10 shows the protection circuit based on N-channel MOSFET devices (N_1 and N_2) with a parallel cross-coupled diode pair (D_3 and D_4) for the ultrasound pulse-echo system. Owing to the gate-source-connected configuration, MOSFET devices have no external bias voltages, eliminating a large gate-source parasitic capacitance and leaving a small parasitic drain-source capacitance [44]. The measured bandwidth, the DC power consumption, the IL, equivalent input noise, recovery time, and total harmonic distortion (THD) were 60 MHz, 26 mW, -5 dB, $2.5 \text{ nV}/\sqrt{\text{Hz}}$, $0.2 \mu\text{s}$, -93 dB, respectively. This protection circuit can provide a lower IL value, lower equivalent input noise, and lower DC power consumption than conventional protection circuits based on a diode limiter configuration.

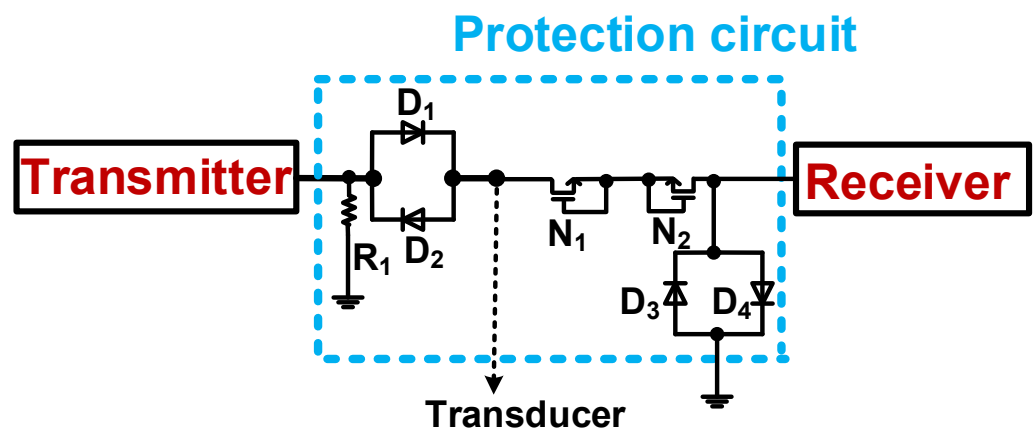


Figure 10. Schematic design of the protection circuit based on gate-source connected MOSFET devices. Adapted with permission from Camacho and Fritsch [44]. Copyright 2008, IEEE.

Figure 11 shows a protection circuit based on a dual-MOSFET device for ultrasound imaging applications. The MOSFET devices (N_1 and N_2) have a high-breakdown voltage tolerance of up to 250 V [45]. In the limiter circuit, there is a gate-source connected to MOSFET with a parallel cross-coupled pair at the outputs of the transmitter and receiver electronics. With this configuration, the signal-to-noise (SNR) was improved from 10 dB to 20 dB. The measured bandwidth, referred-to-input noise, and recovery time with the protection circuit and receiver were 41 MHz, 2 nV/ $\sqrt{\text{Hz}}$, and less than 1 μs , respectively.

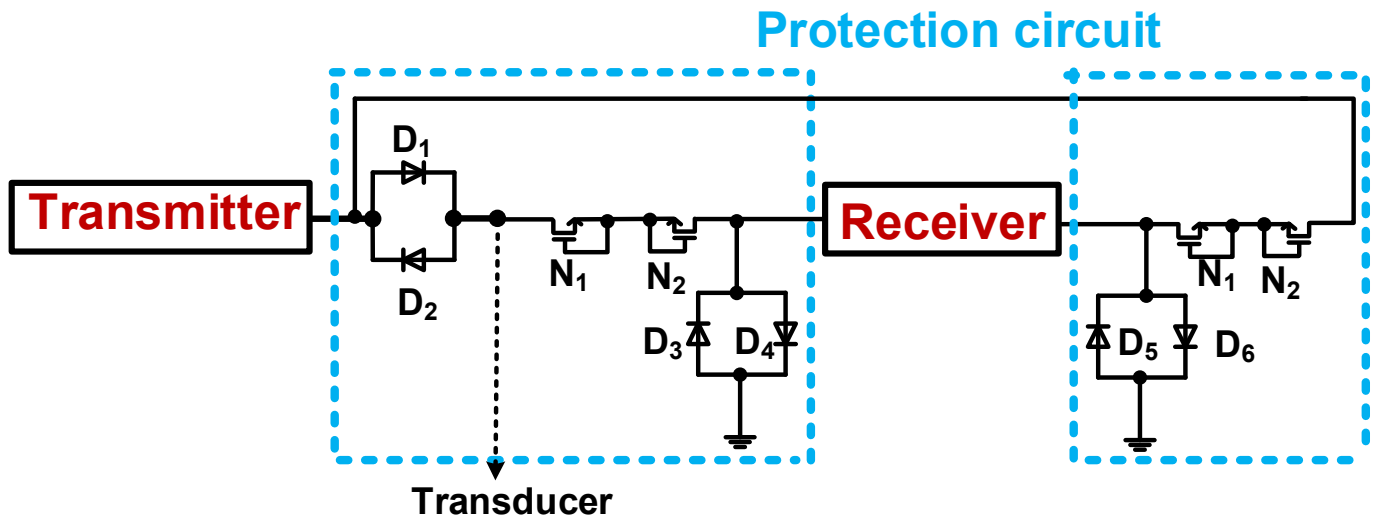


Figure 11. Schematic design of the protection circuit using dual gate-source connected MOSFET device and a parallel cross-coupled pair. Adapted with permission from Chatain et al. [45]. Copyright 2009, IEEE.

Figure 12 shows the protection circuit based on a high-voltage NMOS switch for 50 MHz capacitive micromachined ultrasonic transducer (CMUT) applications [46]. The protection circuit was fabricated using a 0.18 μm complementary MOS (CMOS)/double-diffusion MOS (DMOS) process. During the transmission period, the expanders (D_1 and D_2) are conducted and the switch (N_1) made by the NMOS transistor is turned off because the S_1 clock signal may provide a zero or negative voltage. During the receiving period, the switch is turned on because the S_1 clock signal may provide a positive voltage. This configuration is useful for unipolar pulse transmissions so the chip area can be reduced for multichannel CMUT applications.

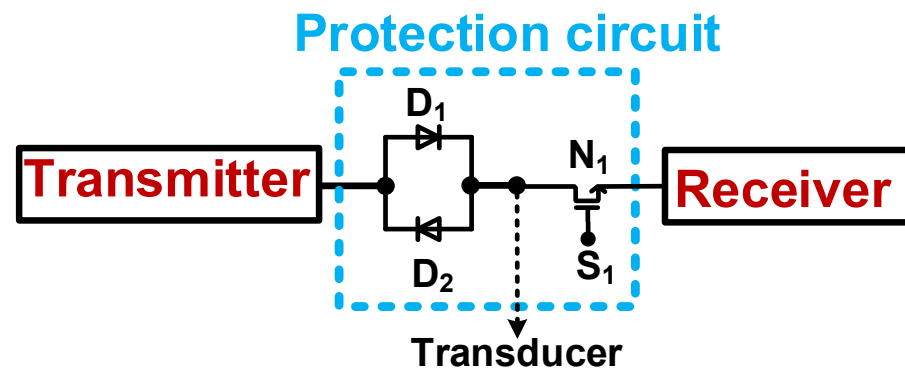


Figure 12. Schematic design of a protection circuit based on a high-voltage switch. Adapted with permission from Zhao et al. [46]. Copyright 2011, IEEE.

Figure 13 shows the protection circuit based on the silicon carbide diode bridge for ultrasound system applications requiring very high voltages above 400 V [47]. Even if the diode bridges (D_3 , D_4 , D_5 , and D_6) do not completely suppress the discharged pulse, the parallel diode pair (D_7 and D_8) can also suppress the pulse. Compared to pin diodes, silicon carbide (SiC) diodes have a faster reverse recovery time, which is usually less than 15 ns [47]. When the positive transmitted pulses reach the bridge diode, the diode (D_5) is turned on, and the positive pulses are suppressed by the diode (D_6). The suppressed positive discharged pulse is directed to the ground via the diode (D_8). When the negative transmitted pulses reach the bridge diode, the diode (D_3) is turned on and the positive pulses are suppressed by the diode (D_4). The suppressed negative discharged pulse is conducted to the ground through the diode (D_7). Like the schematic diagram in Figure 13, the commercial protection circuit like MD0100 also has the same diode bridge configuration [48]. This configuration requires the control to have the fast time of the turn on and off so that we could reduce the ring down of the discharged pulses which should not be combined with the echoes.

The selected resistance values of the resistors (R_1 and R_2) are 1 k Ω and the value of the DC supply voltage (V_{dd}) is 3 V. For the performance of the protection circuit, the measured amplitude of the discharged pulse was approximately 8 V_{p-p} when the voltage applied by the transmitter was 400 V_{p-p} . The measured bandwidth and pulse recovery time were approximately 27 MHz and 25 ns, respectively.

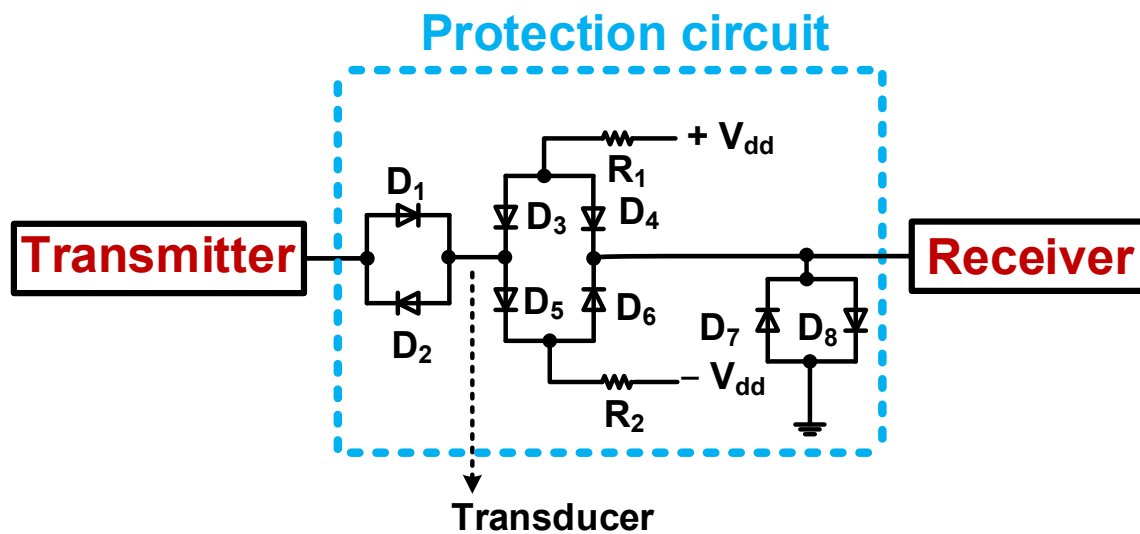


Figure 13. Schematic design of the protection circuit based on a silicon carbide diode bridge configuration.

Figure 14 shows the protection circuit using a bipolar transistor. In comparison to the parallel diode pair in the diode limiter, the developed protection circuit has NPN (N_1 and N_2) and PNP (P_1) bipolar transistors [49]. The positive discharged pulse is routed to the ground through N_1 and N_2 whereas the negative discharged pulse is directed to the ground through P_1 . The developed protection circuit ensures a lower IL and THD. However, the configuration is more complex and is not a cost-effective solution for ultrasound imaging systems that require a multi-array transducer. When a negative pulse of 20 MHz and 50 V_{p-p} was applied, the measured values for IL, THD, NF, bandwidth, and recovery time of the protection circuit were -6.3 dB, -77.3 dB, 9.6 dB, 135 MHz, and 43 ns, respectively.

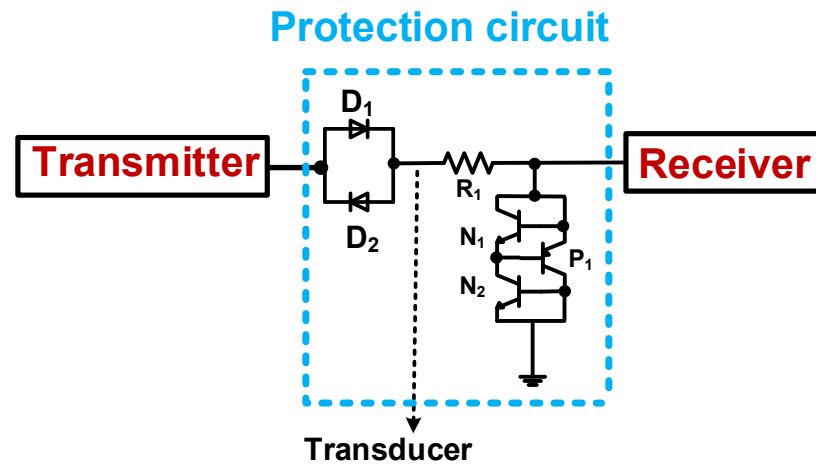


Figure 14. Schematic design of protection circuit using a bipolar transistor. Adapted with permission from Choi et al. [49]. Copyright 2014, Elsevier.

Figure 15 shows a protection circuit for very high-frequency (≥ 100 MHz) ultrasound system applications such as micro-particle stimulation and cell stimulation. To efficiently suppress the noise, two series diode pairs ($D_1, D_2, D_3,$ and D_4) were used as an expander circuit. To reduce the high insertion loss, a limiter circuit consisting of seven gate-drain connected MOSFET with a parallel diode pair was used [50]. The limiter functions as a high-pass filter and is therefore suitable for operating transducers at very high-frequencies owing to its low IL. The measured IL and THD values at 120 MHz were -1.0 dB and -69.89 dB, respectively.

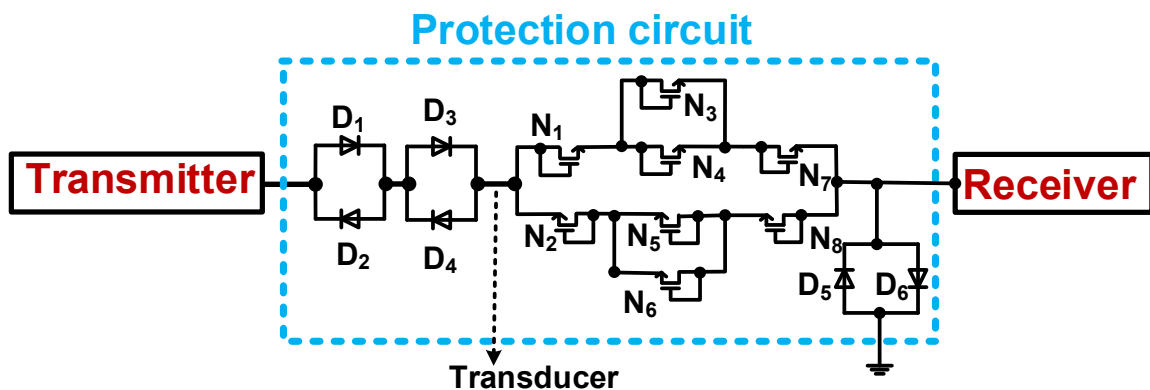


Figure 15. Schematic design of the protection circuit used for the very high-frequency ultrasound system. Adapted with permission from Choi et al. [50]. Copyright 2014, Springer Nature.

Figure 16 shows the protection circuit based on n-channel MOSFET devices. The transmitted pulses were suppressed using two resistors (R_1 and R_2), complementary MOSFET devices (N_3 – N_6), and gate source-connected MOSFET (N_1 and N_2) devices without external power sources [51]. Therefore, this configuration could be useful for impedance adjusting, even when the design is complex and the chip area is large. The echoes from the transducer are passed through a gate-source connected to the MOSFET (N_1 and N_2). The IL and bandwidth of the developed protection circuit are 0.5 dB and 100 MHz, respectively.

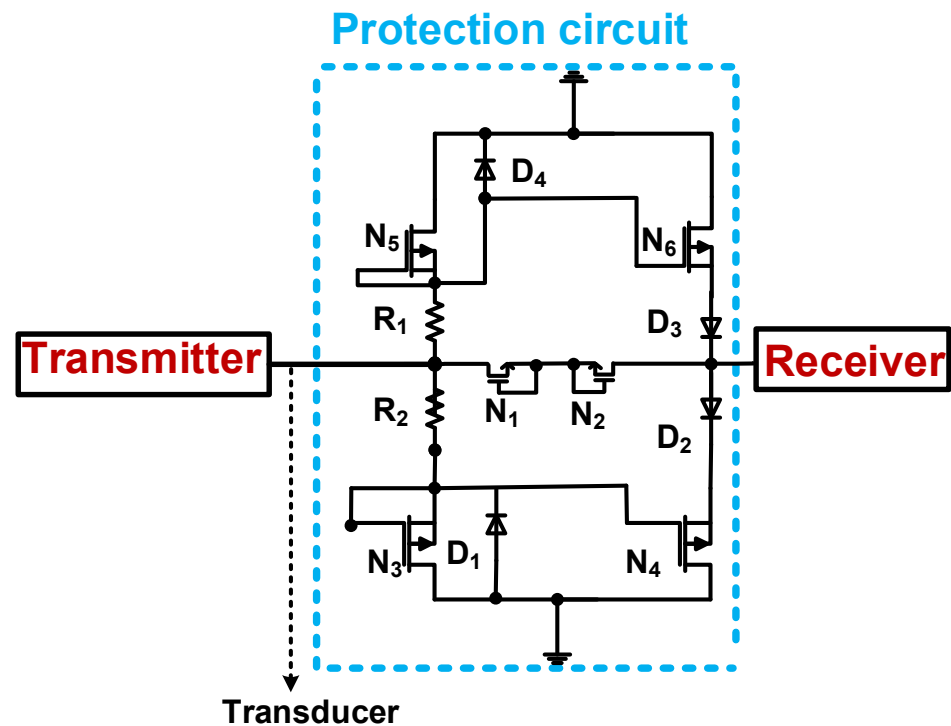


Figure 16. Schematic design of the protection circuit based on the complementary MOSFET and gate-source connected MOSFET devices. Adapted with permission from Hsia [51]. Copyright 2015, IEEE.

There are similar approaches based on gate-source connected MOSFET devices. Gate-source connected MOSFETs with additional gate-source shunt PMOS. The measured IL was 64 dB at 10 MHz. The switches controlled by the PMOS are used to shut down the gate-source connected MOSFETs during the transmitting and receiving times, reducing the static power consumption to 12.1 μW [52]. In addition, the gate-source connected MOSFETs were implemented with a shunt MOSFET to improve the isolation between the transmitting and receiving times for a portable ultrasonic system with a piezoelectric micromachined ultrasonic transducer (PMUT). The simulated IL of the device was 62 dB with a capacitive load of 20 pF [53].

Figure 17 shows a protection circuit that uses a dual-diode limiter to provide a higher discharge pulse for ultrasound system applications. The protection circuit, which is based on a diode limiter, is very simple. Therefore, it is still widely used for laboratory equipment and multichannel ultrasound imaging systems, and different configurations have been developed to improve the suppression capability. Compared to a single-diode limiter, the dual-diode limiter showed higher voltage suppression and faster recovery. When 50 V_{p-p} and 1 MHz pulses were transmitted to the protection circuit, the measured IL, THD, recovering time, and discharge pulse were -3.87 dB, 0.29%, 6.1 μs , and 1.15 V, respectively. The resistance values (R_1 and R_2) were adjusted for impedance matching using a receiver. Compared to the measured discharged pulse and the recovery time of the single diode limiter, the values of the dual diode limiter were improved by 28.69% and 1.61%, respectively.

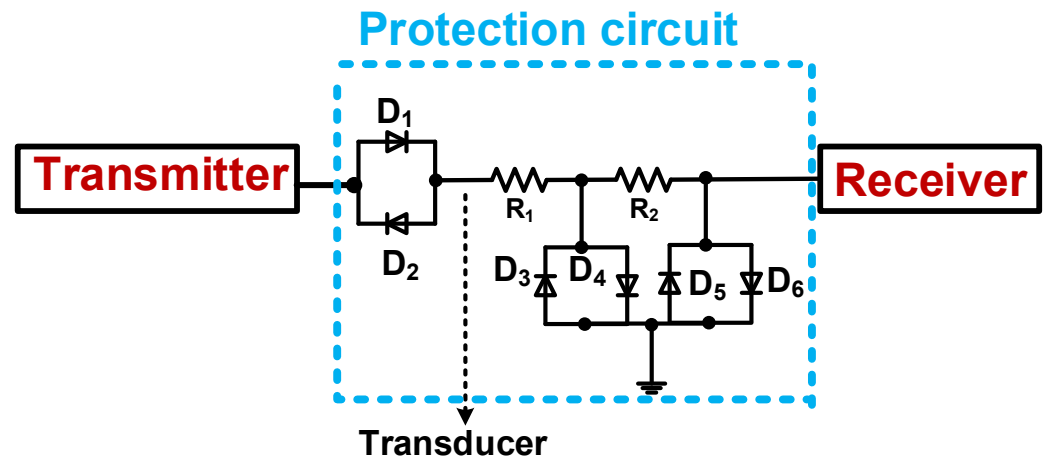


Figure 17. Schematic of the protection circuit with a dual diode limiter. Adapted from Choi, H. [54] with permission under the terms of the CCBY 4.0 License, Copyright 2022, IOS Press.

Ehsanipour et al. have developed a protection circuit that uses a return-to-zero (RTZ) circuit and switch, as shown in Figure 18. This design was developed to save chip space for multichannel ultrasound transducer applications and to improve impedance-matching conditions without any external DC bias voltages [55]. In the designed protection circuit, the n-channel double-diffused MOS (DMOS) transistors (N_2 and N_3), a p-channel DMOS transistor (P_2), and a CMOS transistor (N_0) were used. In high-voltage fabrication, the size of the CMOS transistor (N_0) is significantly smaller than the size of the DMOS transistors (N_2 , N_3 , and P_2), so that the chip die area can be reduced. The obtained discharged pulse voltage and recovery time were 4.5 V and 77.23 ns, respectively.

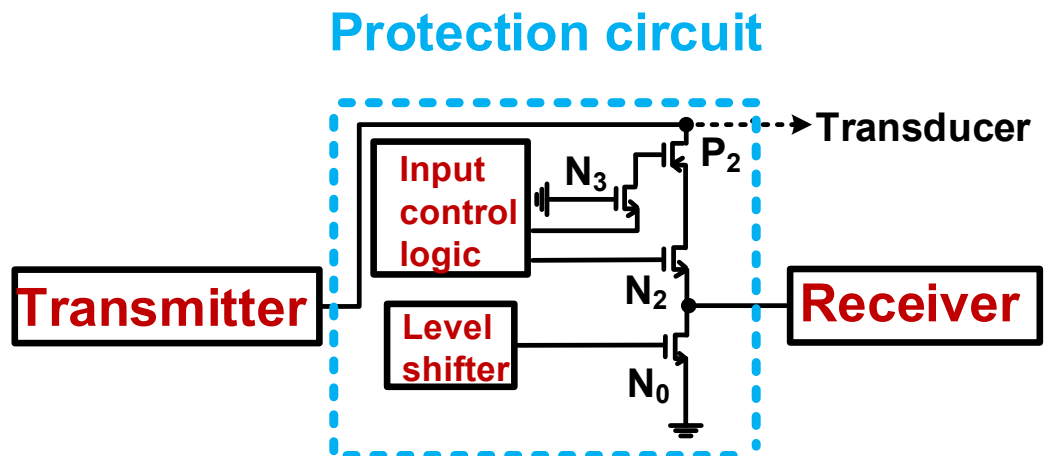


Figure 18. Schematic design of the protection circuit with an RTZ circuit and switch. Adapted with permission from Ehsanipour et al. [55]. Copyright 2023, Wiley.

4. Discussion

High-frequency operation of ultrasound transducers is preferable for IVUS [56,57]. During cell stimulation, a smaller-sized cell-trapping performance can be achieved by increasing the operating frequency of the ultrasound transducer [58]. In IVUS applications, a higher-frequency operation in the ultrasound transducer provides a wider bandwidth and higher lateral resolution [59]. The higher the operating frequency of the piezoelectric materials in an ultrasound transducer, the smaller the piezoelectric materials become [60]. High-amplitude pulsed signals with smaller materials must be used to obtain suitable echo signals [61]. Therefore, protection circuits can be vulnerable in applications operating at higher frequencies. Therefore, proper design of protection circuits is highly desirable.

The protection circuits are typically categorized into three major types: the protection circuits based on a limiter diode, a bridge diode, and MOSFET. Some protection circuits combine these different types of circuits.

A protection circuit based on a diode limiter is easy to implement, but increases the IL at a high frequency operation and thus reduces the bandwidth. The measured IL was 3.87 dB at 1 MHz [54]. Therefore, a protection circuit based on a limiter diode may not be suitable for high-frequency ultrasound transducer applications. However, protection circuits based on a limiter diode are still the most commonly used for ultrasound array imaging systems because of their simple architecture. Therefore, academic researchers still prefer to use protection circuits based on a limiter diode for lab equipment and low-intensity stimulation. However, the high-voltage suppression capability of such a protection circuit based on a limiter diode was no better than that of a protection circuit based on a bridge diode or a MOSFET.

A protection circuit based on a transformer can reduce the IL during high-frequency operation but causes excessive ring-down of the echoes, which may not be suitable for Doppler ultrasound imaging applications that require a long pulse duration. However, it is useful for blocking unwanted DC voltages and adjusting the impedance. Therefore, this configuration is useful for some ultrasound transducers which need to have matching with small impedances. The measured IL value (−4 to −8 dB) at 20 MHz was relatively low [38]. Therefore, the protection circuit based on a transformer may be suitable for high-frequency operation.

The protection circuit based on a bridge diode can provide a low IL at high-frequency operation, but without proper selection of the terminating resistor, it generates a long ring-down and oscillation. In addition, the resistance used to control the bridge diode can significantly affect the impedance, IL, and bandwidth. The measured bandwidth was around 27 MHz [47]. Therefore, a protection circuit based on a bridge diode may not be suitable for high-frequency transducer applications. The bridge diodes must be turned on and off quickly to reduce the ring-down of the discharged pulses. Therefore, the duration of the discharge pulses should not be mixed with the duration of the echoes. The commercial protection circuits also have the same bridge diode configuration to use a control circuit which requires fast turn on and off times. For wearable ultrasound electronics, triboelectric nanogenerators, and energy harvesting circuits—protection circuits based on a bridge diode like commercial protection circuits—have been widely used due to low IL at high-frequency operation [62].

A protection circuit using a MOSFET can provide a low IL and low noise in high-frequency operation. Therefore, high-voltage chip processes have been used to implement protection circuits using MOSFET or high-voltage discrete MOSFET devices. Although high-voltage MOSFET devices offer high-voltage tolerance, they have very large parasitic gate-source, gate-drain, and drain-source capacitances [63–65]. To reduce such unwanted parasitic capacitances, gate source-connected or gate drain-connected MOSFET devices have been used. Compared to the low-voltage chip process, high-voltage MOSFET devices require a very large size [66]. To solve this problem, a protection circuit that uses both low-voltage and high-voltage MOSFETs was used to save space and thus reduce the size of the multi-array ultrasound transducers. The measured IL and equivalent input noises were −5 dB and 2.5 nV/√Hz, respectively [44]. The measured bandwidth and input-referred noise were 41 MHz and 2 nV/√Hz, respectively [45]. The measured IL and bandwidth were 0.5 dB and 100 MHz, respectively [51]. Therefore, the protection circuit based on a MOSFET would be beneficial for high-frequency operation due to low IL and noise performances.

The main parameters of the protection circuit are IL, harmonic distortion, input-referred noise, bandwidth, and recovery time. The IL of the protection circuit was reduced when the operating frequency of the protection circuit was increased. Thus, the high-frequency operation of the ultrasound transducer may be affected by the reduced IL of the protection circuit. A lower IL of the protection circuit may degrade the overall noise performance of the receiver used in the ultrasound system, as the noise figure of the first-stage electronics, such as the protection circuit, mainly determines the overall noise figure of the receiver electronics. This can affect the resolution of the ultrasound systems. The high harmonic distortion of the protection circuit can burden the preamplifier and variable-gain amplifier; therefore, it is desirable for the protection circuit to have a low harmonic distortion. A lower bandwidth of the protection circuit can reduce the echo signal amplitude of the ultrasound transducer. This can be critical for high-frequency ultrasound transducer operations. Therefore, the protection bandwidth must be as wide as possible.

Table 1 gives an overview of the protection circuits developed for ultrasound transducers and system applications. Table 1 lists the types of protection circuits and describes the performance parameters and desired applications.

Table 1. Summary of the protection circuits developed to date for ultrasound applications.

Paper	Type	Performance Parameter	Characteristics	Application
[30]	Transmission line with diode		Advantageous to be matched with the transmitter and receiver when using a certain length of the transmission line.	PVDF ultrasound transducer
[34]	Duplexer design with variable capacitive diode		Reduction in the IL and noise	Ultrasound imaging system
[35]	Transformer with diode		Unwanted DC source blocking.	Ultrasound imaging system
[38]	Wideband transformer-based limiter	IL is -4 to -8 dB at 20 MHz and -55 to -66 dB at 45 MHz.	Wideband transformers can improve IL at high-frequency operation.	Ultrasound imaging system
[39]	Bridge diode		Using a transmission line improves impedance matching.	High-frequency ultrasound skin imaging
[42]	Dual bridge diode		Advantageous for impedance matching and the input and output receiver.	Ultrasound catheter
[43]	Metal-oxide-semiconductor field-effect transistor (MOSFET) shunt device	IL is -19.17 dB	Chip area reduction using low-voltage switch circuit for high-channel system	Portable high-channel ultrasound imaging system
[44]	Gate-source connected MOSFET device	IL, total harmonic distortion (THD), bandwidth, input-referred noise, recovering time, and power consumption are -5 dB, -93 dB, 60 MHz, 2.5 nV/ $\sqrt{\text{Hz}}$, 0.2 μs , and 26 mW, respectively.	Improvement of IL, noise, and DC power consumption.	Ultrasound pulse-echo system

Table 1. Cont.

Paper	Type	Performance Parameter	Characteristics	Application
[45]	Dual gate-source connected MOSFET device	Bandwidth, input-referred noise, and recovering time are 41 MHz, 2 nV/ $\sqrt{\text{Hz}}$, and <1 μs , respectively.	Signal-to-noise ratio improvement in deeper depth	Ultrasound imaging system
[46]	N-channel MOSFET switch		Useful for unipolar pulse transmission and chip area reduction	Capacitive micromachined ultrasonic transducer
[47]	Bridge diode based on SiC diode	Bandwidth and recovering time are 27 MHz and 25 ns.	Useful for very-high-voltage above 400 V transmission	Very-high-voltage ultrasound system
[49]	Bipolar-transistor	IL, THD, bandwidth, input-referred noise, and recovering time are 6.3 dB, -77.3 dB, 135 MHz, 96 dB, and 43 ns, respectively.	Useful to lower IL and THD for high-frequency operation	High-frequency ultrasound transducer
[50]	Gate-drain connected MOSFET device	IL and THD are -1.0 dB and -69.89 dB at 120 MHz, respectively.	Useful for improving IL for very high-frequency transducer	High-frequency ultrasound imaging system
[51]	Complementary and gate-source connected MOSFET device	IL and bandwidth are -0.5 dB and 100 MHz, respectively.	Useful for impedance matching without external DC bias	Very high-frequency ultrasound transducer
[52]	Gate-source connected MOSFET switch	Static power consumption is 12.1 μW .	Useful for lowering static power consumption	Ultrasound imaging system
[54]	Diode limiter	IL, THD, and recovering time are -3.87 dB, 0.29%, and 6.1 μs .	Improved sensitivity with conventional diode limiter design	Multi-channel ultrasound transducer
[55]	RTZ circuit and switch	The recovery time is 77.23 ns.	Chip area reduction using a low-voltage switch circuit	Ultrasound imaging system

Table 2 summarizes the contribution and limitation of the currently developed three major types of protection circuits. Therefore, academic researchers and system designers can appropriately select the types of protection circuits to optimize the performance of ultrasound transducers or systems.

Table 2. Contribution and limitation of the currently developed protection circuits.

Type	Contribution	Limitation
Protection circuits based on a limiter diode	Useful for array imaging systems due to simple architecture	High IL at high frequency
Protection circuits based on a bridge diode	Low IL at high frequency	Required to control fast turn-on and off time
Protection circuits based on a MOSFET	Low IL and low noise at high frequency	To reduce space, the chip process needs to be used

5. Conclusions

High- and very high-frequency ultrasound transducers have a low sensitivity. Therefore, transmit pulses with high amplitude voltage or power signals must be used to trigger the ultrasound transducers. Therefore, a protection circuit may affect the performance of the ultrasound transducer. However, there are no review articles describing the proper selection of protection circuits for ultrasound transducers and system applications. Therefore,

the design topology and specifications of protection circuits for ultrasound transducers used in ultrasound transducer, imaging, and stimulation applications are reviewed. The protection circuit consists of expander and limiter circuits. The expander usually consists of a single series-crossed coupled pair and is used to suppress the ring-down of the transmitted high-voltage pulses, whereas the limiter is used to minimize IL while suppressing the high-voltage pulses. In particular, a protection circuit must be designed considering a low IL and wide bandwidth to avoid the suppression of the low-amplitude echo signal generated by high-frequency or very high-frequency ultrasound transducers. In this review, a specific design topology and suitable applications have been proposed. Therefore, this review paper will help academic ultrasound researchers and ultrasound system engineers to design or use protection circuits.

Funding: This work was supported by the National Research Foundation of Korea (NRF) grant funded by the Korea government (MSIT) (no. 2020R1A2C4001606).

Conflicts of Interest: The author declares no conflicts of interest.

Abbreviations

AC	Alternating current
ADC	Analog-to-digital converter
CMOS	Complementary MOS
CMUT	Capacitive micromachined ultrasonic transducer
DAC	Digital-to-analog converter
DC	Direct current
DMOS	Double-diffused MOS
ESD	Electro-static discharge
HD2	Second harmonic distortion
HD3	Third harmonic distortion
IL	Insertion loss
IVUS	Intravascular ultrasound
MOS	Metal-oxide-semiconductor
MOSFET	Metal-oxide-semiconductor field-effect transistor
NF	Noise figure
NMOS	N-channel MOS
PMOS	P-channel MOS
PMUT	Piezoelectric micromachined ultrasonic transducer
PVDF	Polyvinylidene
RTZ	Return-to-zero
SNR	Signal-to-noise ratio
THD	Total harmonic distortion

References

1. Fenster, A. *3D Ultrasound Devices, Applications, and Algorithms*; CRC Press: Boca Raton, FL, USA, 2023.
2. Mattoon, J.S.; Sellon, R.K.; Berry, C.R. *Small Animal Diagnostic Ultrasound*; Elsevier Health Sciences: Amsterdam, The Netherlands, 2020.
3. He, Z.; Zheng, F.; Ma, Y.; Kim, H.H.; Zhou, Q.; Shung, K.K. A sidelobe suppressing near-field beamforming approach for ultrasound array imaging. *J. Acoust. Soc. Am.* **2015**, *137*, 2785–2790. [[CrossRef](#)] [[PubMed](#)]
4. Zhou, Q.; Lau, S.; Wu, D.; Shung, K.K. Piezoelectric films for high frequency ultrasonic transducers in biomedical applications. *Prog. Mater. Sci.* **2010**, *56*, 139–174. [[CrossRef](#)] [[PubMed](#)]
5. Qiu, W.; Wang, C.; Li, Y.; Zhou, J.; Yang, G.; Xiao, Y.; Feng, G.; Jin, Q.; Mu, P.; Qian, M.; et al. A scanning-mode 2D shear wave imaging (s2D-SWI) system for ultrasound elastography. *Ultrasonics* **2015**, *62*, 89–96. [[CrossRef](#)] [[PubMed](#)]
6. Zhang, T.; Yuan, J.; Li, J.; Li, W.; Qin, Y.; Ge, X.; Ou-Yang, J.; Yang, X.; Zhu, B. Design and prediction of laser-induced damage threshold of CNT-PDMS optoacoustic transducer. *Ultrasonics* **2024**, *142*, 107377. [[CrossRef](#)] [[PubMed](#)]

7. Lin, R.; Zhang, Q.; Lv, S.; Zhang, J.; Wang, X.; Shi, D.; Gong, X.; Lam, K. Miniature intravascular photoacoustic endoscopy with coaxial excitation and detection. *J. Biophotonics* **2023**, *16*, e202200269. [[CrossRef](#)] [[PubMed](#)]
8. Kripfgans, O.D.; Chan, H.-L. *Ultrasonic Imaging: Physics and Mechanism*; Springer International Publishing: Berlin, Germany, 2021.
9. Qiu, W.; Yu, Y.; Chabok, H.R.; Liu, C.; Tsang, F.K.; Zhou, Q.; Shung, K.K.; Zheng, H.; Sun, L.A. Flexible Annular-Array Imaging Platform for Micro-Ultrasound. *IEEE Trans. Ultrason. Ferroelectr. Freq. Control* **2013**, *60*, 178–186. [[PubMed](#)]
10. Nakamura, K. *Ultrasonic Transducers: Materials and Design for Sensors, Actuators and Medical Applications*; Elsevier: Amsterdam, The Netherlands, 2012.
11. Weibao, Q.; Yanyan, Y.; Keung, T.F.; Lei, S. A multifunctional, reconfigurable pulse generator for high-frequency ultrasound imaging. *IEEE Trans. Ultrason. Ferroelectr. Freq. Control* **2012**, *59*, 1558–1567. [[CrossRef](#)] [[PubMed](#)]
12. Qiao, Y.; Zhang, X.; Zhang, G. Acoustic radiation force on a fluid cylindrical particle immersed in water near an impedance boundary. *J. Acoust. Soc. Am.* **2017**, *141*, 4633–4641. [[CrossRef](#)]
13. Zhou, Q.; Lam, K.H.; Zheng, H.; Qiu, W.; Shung, K.K. Piezoelectric single crystal ultrasonic transducers for biomedical applications. *Prog. Mater. Sci.* **2014**, *66*, 87–111. [[CrossRef](#)]
14. Shung, K.K. *Diagnostic Ultrasound: Imaging and Blood Flow Measurements*; Taylor & Francis: Boca Raton, FL, USA, 2015.
15. Choi, H. Power Amplifier Design for Ultrasound Applications. *Micromachines* **2023**, *14*, 1342. [[CrossRef](#)] [[PubMed](#)]
16. Jung, U.; Choi, J.H.; Choo, H.T.; Kim, G.U.; Ryu, J.; Choi, H. Fully Customized Photoacoustic System Using Doubly Q-Switched Nd:YAG Laser and Multiple Axes Stages for Laboratory Applications. *Sensors* **2022**, *22*, 2621. [[CrossRef](#)] [[PubMed](#)]
17. Choi, H.; Shung, K.K. Novel power MOSFET-based expander for high frequency ultrasound systems. *Ultrasonics* **2014**, *54*, 121–130. [[CrossRef](#)] [[PubMed](#)]
18. Bugg, D.V. *Electronics: Circuits, Amplifiers and Gates*; CRC Press: Boca Raton, FL, USA, 2021.
19. Kim, K.; Choi, H. High-efficiency high-voltage class F amplifier for high-frequency wireless ultrasound systems. *PLoS ONE* **2021**, *16*, e0249034. [[CrossRef](#)] [[PubMed](#)]
20. Choi, H. Harmonic-Reduced Bias Circuit for Ultrasound Transducers. *Sensors* **2023**, *23*, 4438. [[CrossRef](#)]
21. Razavi, B. *Design of Analog CMOS Integrated Circuits*; McGraw-Hill Science: New York, NJ, USA, 2016.
22. Kim, K.; Choi, H. A New Approach to Power Efficiency Improvement of Ultrasonic Transmitters via a Dynamic Bias Technique. *Sensors* **2021**, *21*, 2795. [[CrossRef](#)] [[PubMed](#)]
23. Ozenbaugh, R.L.; Pullen, T.M. *EMI Filter Design*; CRC Press: Boca Raton, FL, USA, 2016.
24. Irwin, J.D.; Nelms, R.M. *Basic Engineering Circuit Analysis*; John Wiley & Sons: Hoboken, NJ, USA, 2020.
25. Choi, H. An Inverse Class-E Power Amplifier for Ultrasound Transducer. *Sensors* **2023**, *23*, 3466. [[CrossRef](#)] [[PubMed](#)]
26. Chen, W.-K. *The Circuits and Filters Handbook*; CRC Press: Boca Raton, FL, USA, 2002.
27. Pedroni, V.A. *Circuit Design with VHDL*; MIT Press: Cambridge, MA, USA, 2020.
28. Choi, H.; Yoon, C.; Yeom, J.-Y. A Wideband High-Voltage Power Amplifier Post-Linearizer for Medical Ultrasound Transducers. *Appl. Sci.* **2017**, *7*, 354. [[CrossRef](#)]
29. Choi, H. Design of Preamplifier for Ultrasound Transducers. *Sensors* **2024**, *24*, 786. [[CrossRef](#)]
30. Lockwood, G.; Hunt, J.; Foster, F. The design of protection circuitry for high-frequency ultrasound imaging systems. *IEEE Trans. Ultrason. Ferroelectr. Freq. Control* **1991**, *38*, 48–55. [[CrossRef](#)]
31. Rothwell, E.J.; Cloud, M.J. *Electromagnetics*; CRC Press: Boca Raton, FL, USA, 2018.
32. Bera, S.C. *Microwave High Power High Efficiency GaN Amplifiers for Communication*; Springer Nature: Dordrecht, The Netherlands, 2022.
33. Postema, M. *Fundamentals of Medical Ultrasound*; Taylor and Francis: New York, NJ, USA, 2011.
34. Oppelt, R.; Vester, M. Duplexer Including a Variable Capacitance Diode for an Ultrasound Imaging System. U.S. Patent 5,609,154, 11 March 1997.
35. Oppelt, R.; Petersen, D.A. Ultrasound Front-End Circuit Combining the Transmitter and Automatic Transmit/Receiver Switch. U.S. Patent 6,083,164, 4 July 2000.
36. Rahmani-Andebili, M. *Advanced Electrical Circuit Analysis*; Springer Nature: Dordrecht, The Netherlands, 2022.
37. Sevic, J.F. *The Load-Pull Method of RF and Microwave Power Amplifier Design*; Wiley: Hoboken, NJ, USA, 2020.
38. Poulsen, J. Low loss wideband protection circuit for high frequency ultrasound. In Proceedings of the IEEE Ultrasonics Symposium, Tahoe, NV, USA, 17–20 October 1999; Volume 1, pp. 823–826.
39. Vogt, M.; Paul, B.; Scharenberg, S.; Scharenberg, R.; Ermert, H. Development of a high frequency ultrasound skin imaging system: Optimization utilizing time domain reflectometry and network analysis. In Proceedings of the IEEE Symposium on Ultrasonics, Honolulu, HI, USA, 5–8 October 2003; Volume 1, pp. 744–747.
40. Suetens, P. *Fundamentals of Medical Imaging*; Cambridge University Press: Cambridge, UK, 2017.
41. Wang, L.V.; Wu, H.-I.; Masters, B.R. *Biomedical Optics, Principles and Imaging*; John Wiley & Sons: Hoboken, NJ, USA, 2012.
42. Moore, T.C.; Suorsa, V.; Masters, D. Preamplifier and Protection Circuit for an Ultrasound Catheter. USA Patent 6,511,432 B2, 28 January 2003.

43. Fuller, M.I.; Blalock, T.N.; Hossack, J.A.; Walker, W.F. Novel transmit protection scheme for ultrasound systems. *IEEE Trans. Ultrason. Ferroelectr. Freq. Control* **2006**, *54*, 79–86. [[CrossRef](#)] [[PubMed](#)]
44. Camacho, J.; Fritsch, C. Protection circuits for ultrasound applications. *IEEE Trans. Ultrason. Ferroelectr. Freq. Control* **2008**, *55*, 1160–1164. [[CrossRef](#)] [[PubMed](#)]
45. Chatain, P.; Voisin, D.; Legros, M.; Ferin, G.; Dufait, R. Improving ultrasound imaging with integrated electronics. In Proceedings of the 2009 IEEE International Ultrasonics Symposium, Rome, Italy, 20–23 September 2009; pp. 2718–2721.
46. Zhao, D.; Tan, M.T.; Cha, H.-K.; Qu, J.; Mei, Y.; Yu, H.; Basu, A.; Je, M. High-voltage pulser for ultrasound medical imaging applications. In Proceedings of the 2011 International Symposium on Integrated Circuits (ISIC), Singapore, 12–14 December 2011; pp. 408–411.
47. Zhou, S.Y.; Zhang, K.; Xiao, D.; Xu, C.G.; Yang, B. Application of Silicon Carbide Diode in Ultrasound High Voltage Pulse Protection Circuit. *Appl. Mech. Mater.* **2013**, *290*, 115–119. [[CrossRef](#)]
48. MD0100. Available online: <https://www.microchip.com/en-us/product/md0100> (accessed on 13 February 2025).
49. Choi, H.; Yang, H.-C.; Shung, K.K. Bipolar-power-transistor-based limiter for high frequency ultrasound imaging systems. *Ultrasonics* **2013**, *54*, 754–758. [[CrossRef](#)]
50. Choi, H.; Shung, K.K. Protection Circuits for Very High Frequency Ultrasound Systems. *J. Med. Syst.* **2014**, *38*, 34. [[CrossRef](#)] [[PubMed](#)]
51. Hsia, C. Design of a power-less integrated protection circuit for biomedical ultrasound transmit/receive. In Proceedings of the 2015 IEEE International Conference on Consumer Electronics—Taiwan (ICCE-TW), Taipei, Taiwan, 6–8 June 2015; pp. 184–185.
52. Kajiyama, S.; Igarashi, Y.; Yazaki, T.; Katsube, Y.; Nishimoto, T.; Nakagawa, T.; Nakamura, Y.; Hayashi, Y.; Kaneko, T.; Ishikuro, H.; et al. T/R Switch Composed of Three HV-MOSFETs With 12.1- μ W Consumption That Enables Per-Channel Self-Loopback AC Tests and -18.1 -dB Switching Noise Suppression for 3-D Ultrasound Imaging With 3072-Ch Transceiver. *IEEE Trans. Very Large Scale Integr. Syst.* **2021**, *30*, 153–165. [[CrossRef](#)]
53. Zhang, Y.; Jiang, D.; Demosthenous, A. A Differential SPDT T/R Switch for PMUT Biomedical Ultrasound Systems. In Proceedings of the 2024 IEEE International Symposium on Circuits and Systems (ISCAS), Singapore, 19–22 May 2024; pp. 1–4.
54. Choi, H. Novel dual-resistor-diode limiter circuit structures for high-voltage reliable ultrasound receiver systems. *Technol. Health Care* **2022**, *30*, 513–520. [[CrossRef](#)] [[PubMed](#)]
55. Ehsanipour, R.; Shoaie, O. A compact bipolar high-voltage pulser with a novel transistor gate–source protection scheme for ultrasound imaging applications. *Int. J. Circuit Theory Appl.* **2023**, *52*, 2097–2109. [[CrossRef](#)]
56. Zhang, T.; Liang, H.; Wang, Z.; Qiu, C.; Peng, Y.B.; Zhu, X.; Li, J.; Ge, X.; Xu, J.; Huang, X.; et al. Piezoelectric ultrasound energy-harvesting device for deep brain stimulation and analgesia applications. *Sci. Adv.* **2022**, *8*, eabk0159. [[CrossRef](#)]
57. Li, J.; Ma, Y.; Zhang, T.; Shung, K.K.; Zhu, B. Recent Advancements in Ultrasound Transducer: From Material Strategies to Biomedical Applications. *BME Front.* **2022**, *2022*, 9764501. [[CrossRef](#)] [[PubMed](#)]
58. Zeng, Y.; Hao, J.; Zhang, J.; Jiang, L.; Youn, S.; Lu, G.; Yan, D.; Kang, H.; Sun, Y.; Shung, K.K.; et al. Manipulation and Mechanical Deformation of Leukemia Cells by High-Frequency Ultrasound Single Beam. *IEEE Trans. Ultrason. Ferroelectr. Freq. Control* **2022**, *69*, 1889–1897. [[CrossRef](#)] [[PubMed](#)]
59. Qiu, W.; Wang, X.; Chen, Y.; Fu, Q.; Su, M.; Zhang, L.; Xia, J.; Dai, J.; Zhang, Y.; Zheng, H. Modulated Excitation Imaging System for Intravascular Ultrasound. *IEEE Trans. Biomed. Eng.* **2016**, *64*, 1935–1942. [[CrossRef](#)]
60. You, K.; Kim, S.-H.; Choi, H. A Class-J Power Amplifier Implementation for Ultrasound Device Applications. *Sensors* **2020**, *20*, 2273. [[CrossRef](#)]
61. Safari, A.; Akdogan, E.K. *Piezoelectric and Acoustic Materials for Transducer Applications*; Springer Science & Business Media: Berlin, Germany, 2008.
62. Zhou, Y.; Zhang, S.X.; Li, G.P. Piezoelectric Nuclear Battery Driven by the Jet-Flow. In Proceedings of the 2017 25th International Conference on Nuclear Engineering, Shanghai, China, 2–6 July 2017.
63. Kazimierzczuk, M.K. *RF Power Amplifier*; John Wiley & Sons: Hoboken, NJ, USA, 2014.
64. Gurevich, V. *Protection Devices and Systems for High-Voltage Applications—Book Review*; CRC Press: Boca Raton, FL, USA, 2003.
65. Su, M.; Zhang, Z.; Hong, J.; Huang, Y.; Mu, P.; Yu, Y.; Liu, R.; Liang, S.; Zheng, H.; Qiu, W. Cable-Shared Dual-Frequency Catheter for Intravascular Ultrasound. *IEEE Trans. Ultrason. Ferroelectr. Freq. Control* **2019**, *66*, 849–856. [[CrossRef](#)] [[PubMed](#)]
66. Middleman, S.; Hochberg, A.K. *Process Engineering Analysis in Semiconductor Device Fabrication*; McGraw-Hill Education: New York, NJ, USA, 1993.

Disclaimer/Publisher’s Note: The statements, opinions and data contained in all publications are solely those of the individual author(s) and contributor(s) and not of MDPI and/or the editor(s). MDPI and/or the editor(s) disclaim responsibility for any injury to people or property resulting from any ideas, methods, instructions or products referred to in the content.